

**Supplemental Figures for**

**Birth of protein-coding exons by ancient domestication of LINE-1 retrotransposon**

Koichi Kitao, Kenji Ichianagi, So Nakagawa

**Table of Contents:**

Figure S1. An alignment of Lyosin-like proteins obtained from NCBI BLASTP search.

Figure S2. Mutations causing the ORF truncation of Lyosin exon L.

Figure S3. Analysis of the nonsynonymous and synonymous codon substitution ( $d_N/d_S$ ) ratio.

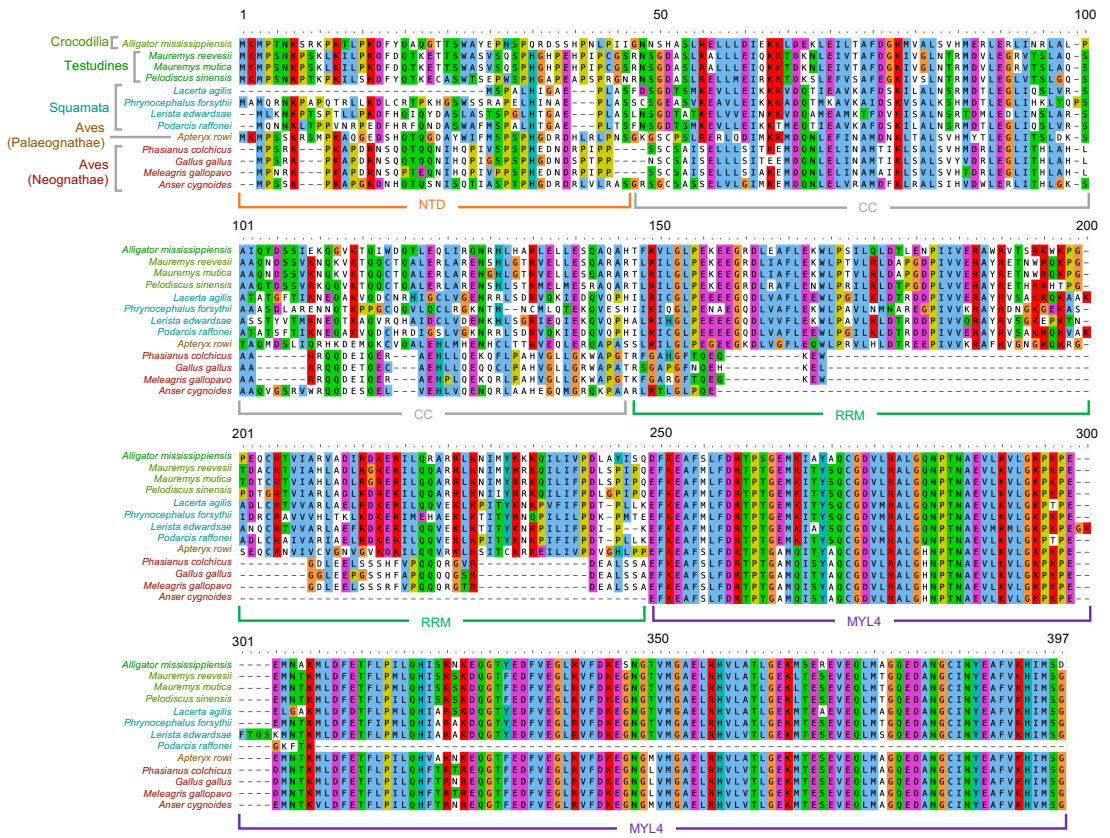
Figure S4. Tissue expression of the *Lyosin* transcript in the American alligator and Chinese soft-shelled turtle.

Figure S5. Other genes with ORF1p-like isoforms.

Figure S6. No overlap between the L1 ORF1 exon and de novo predicted repeats by RepeatModeler2.

Figure S7. Transcription factor binding sites of the *MYL4* and *Lyosin* isoforms.

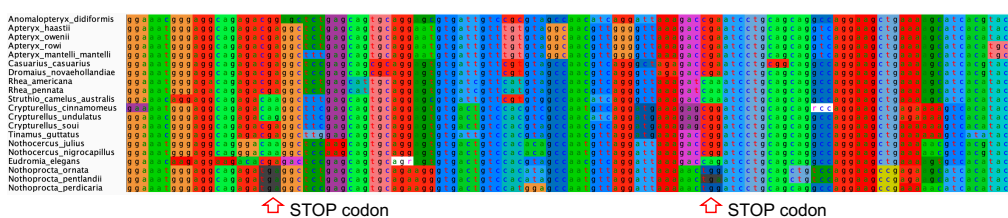
Figure S8. A canonical exon of *UNC13C* encodes a protein similar to L1 ORF1p.



**Figure S1. An alignment of Lysoin-like proteins obtained from NCBI BLASTP search.** The accession numbers of the proteins were listed in **Dataset S1**.

**A**

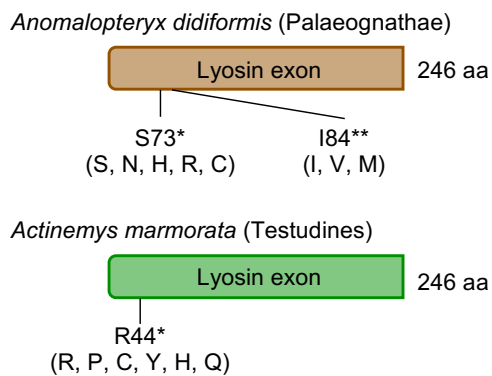
| Species                       | Genome            | Clade           | Mutations   |
|-------------------------------|-------------------|-----------------|---|
| <i>Nothoprocta ornata</i>     | GCA_5F013398335.1 | Palaeognathae   | nonsense mutation   |
| <i>Nothoprocta pentlandii</i> | GCA_5F013398315.1 | Palaeognathae   | nonsense mutation (2)                                       |
| <i>Nothoprocta perdicaria</i> | GCF_5F003342845.1 | Palaeognathae   | nonsense mutation   |
| <i>Casuarius casuarius</i>    | GCA_5F003342895.1 | Palaeognathae   | deletion (1 base)   |
| <i>Rafetus swinhoei</i>       | GCA_5F019425775.1 | Testudines      | deletion (1 base)   |
| <i>Sphenodon punctatus</i>    | GCA_5F003113815.1 | Rhynchocephalia | deletion (1 base)   |
| <i>Varanus komodoensis</i>    | GCF_5F004798865.1 | Squamata        | nonsense mutation, deletion (2 bases), insertion (23 bases) |

**B**

**Figure S2. Mutations causing the ORF truncation of Lyosin exon L.** (A) Summary of mutations observed in the species where the intact exon L was not detected despite positive hit on the BLAT search. (B) A shared nonsense mutation ("tag" stop codon) in the genus *Nothoprocta* (left arrow) and an additional species-specific nonsense mutation (right arrow).

**A**

|               | No. of species | $d_N/d_S$ | M0          |                 | M1 versus M2 |                 | M7 versus M8 |    | No. of positive selection sites |  |
|---------------|----------------|-----------|-------------|-----------------|--------------|-----------------|--------------|----|---------------------------------|--|
|               |                |           | $2\Delta L$ | <i>p</i> -value | $2\Delta l$  | <i>p</i> -value | M2           | M8 |                                 |  |
| Palaeognathae | 15             | 0.5188    | 10.0666     | 0.0065          | 12.6683      | 0.0018          | 1            | 2  |                                 |  |
| Crocodilia    | 4              | 1.2181    | 1.5544      | 0.4597          | 1.5544       | 0.4597          | 0            | 0  |                                 |  |
| Testudines    | 23             | 0.4116    | 0.0000      | 1.0000          | 8.1628       | 0.0169          | 0            | 1  |                                 |  |
| Squamata      | 14             | 0.5351    | 0.0321      | 0.9841          | 4.4942       | 0.1057          | 0            | 0  |                                 |  |

**B**

**Figure S3. Analysis of the nonsynonymous and synonymous codon substitution ( $d_N/d_S$ ) ratio.** (A)  $2\Delta L$  indicates a two-fold difference in the natural log values of the maximum likelihood ratio from pairwise comparisons of the different models. The *p*-value indicates the confidence in rejecting the natural models (M1a or M7) in favor of the positive selection model (M2a or M8) using Pearson's chi-squared test. Codons under positive selection were identified with a posterior probability of 95% by Bayes empirical Bayes (BEB) analysis in M8. (B) The sites under positive selection were illustrated based on the Lyosin exon L of representative species. Amino acids other than the representative sequences were shown in brackets. \*: supported in M8 model, \*\*: supported in M2 and M8 models.

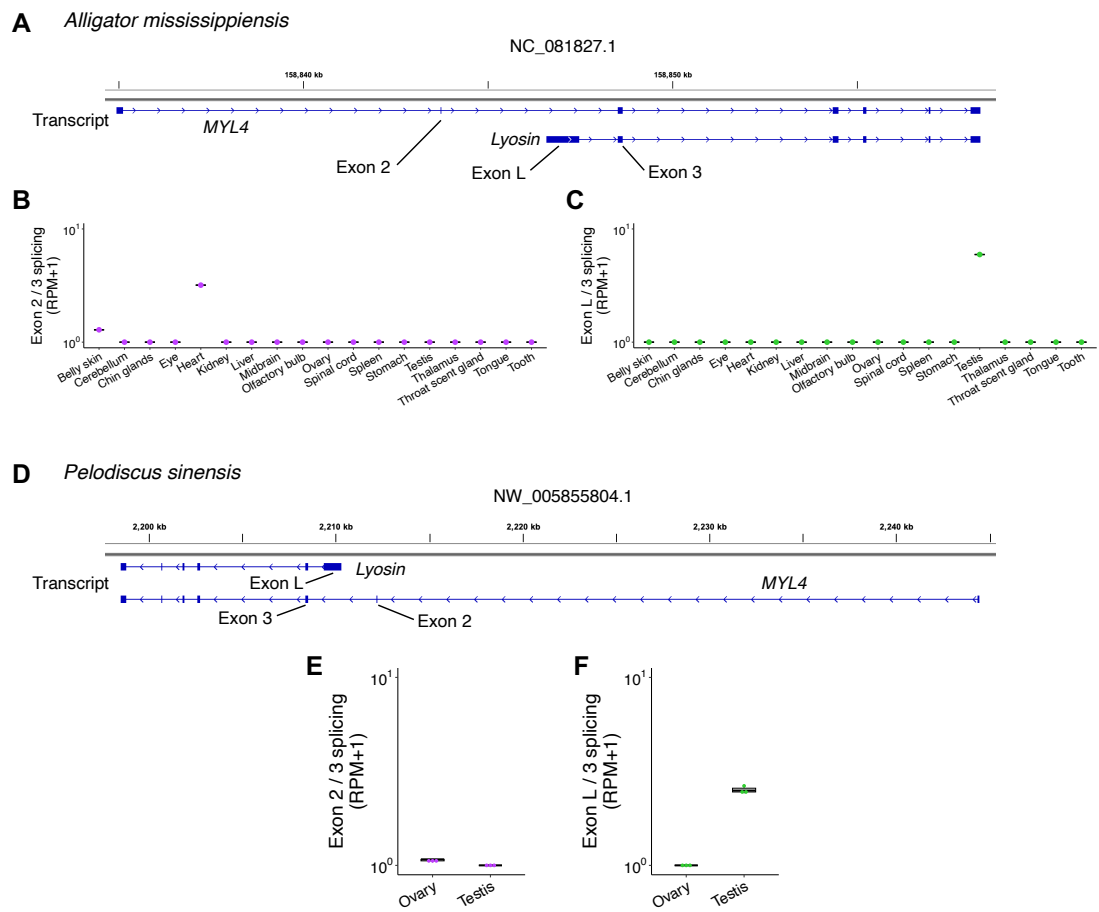


**Figure S4. Tissue expression of the Lyosin transcript in the American alligator and Chinese soft-shelled turtle.** (A) Genome browser view of the *MYL4* gene in American alligator (*Alligator mississippiensis*). The blue lines represent the assembled transcripts by RNA-seq. (B and C) Box plot and point representations of splice junction reads spanning exon 2 to 3 (B) and exon L to 3 (C) of the *MYL4* gene in American alligator (*Alligator mississippiensis*). (D-E) The genome browser view and the normalized number of splice junction reads in Chinese soft-shelled turtle (*Pelodiscus sinensis*). RPM, reads per million.

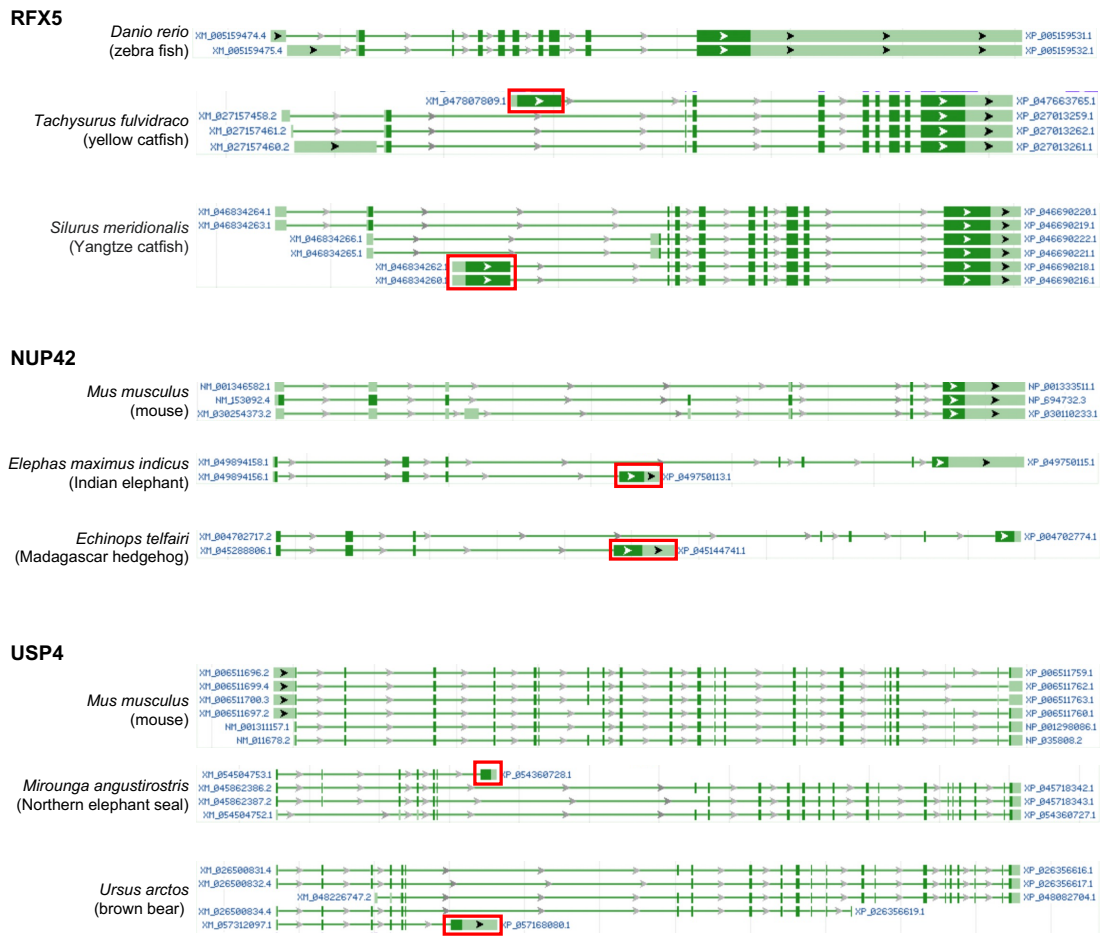


**Figure S5. Other genes with ORF1p-like isoforms.** Screenshots from the NCBI gene browser. The squared exons are non-canonical alternative exons encoding ORF1p-like proteins.

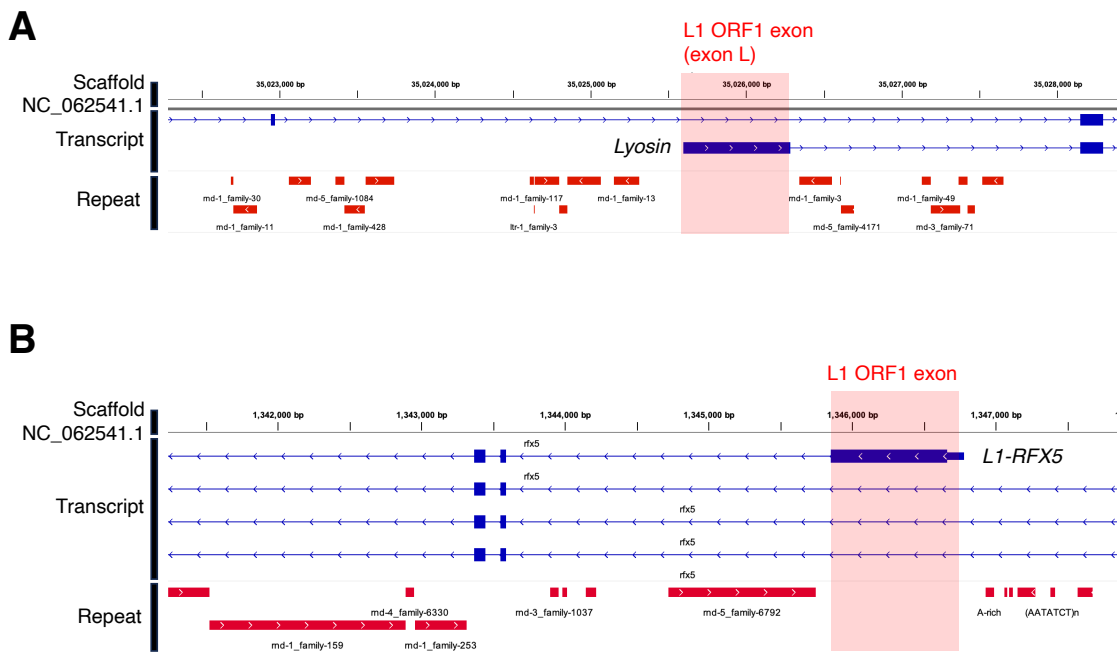


**Figure S6. No overlap between the L1 ORF1 exon and de novo predicted repeats by RepeatModeler2.** (A) The genome browser view of *Lyosin* exon L in green anole (*Anolis carolinensis*). The blue lines indicate the transcripts of the *MYL4* gene. The repeat consensus sequence was constructed by RepeatModeler version 2.0.4 with "-LTRStruct" option. RepeatMasker version 4.1.5 was used for masking the genome assembly with the constructed repeat consensus sequences. (B) The genome browser view of *L1-RFX5* and repeat sequences in *Tachysurus fulvidraco*.

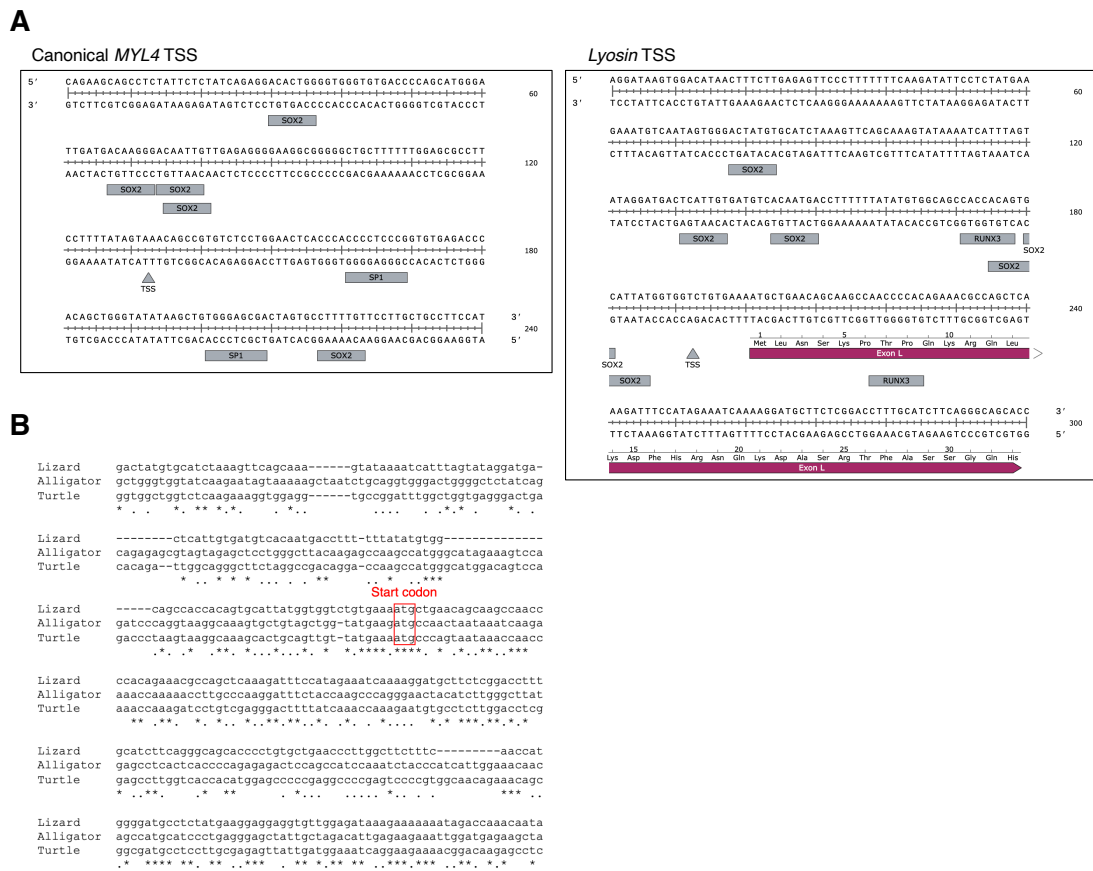


**Figure S7. Transcription factor binding sites of the *MYL4* and *Lyosin* isoforms.** (A) The transcription binding sites were mapped by the JASPAR database (<https://jaspar.elixir.no/>) using the latest version of *Homo sapiens* of RUNX3 (ID: MA0684.3), SP1 (ID: MA0079.5), SOX2 (ID: MA0143.5), and YY1 (ID: MA0095.2) in the Transcription start site (TSS) of *Anolis carolinensis* *MYL4* and *Lyosin*. TSS was inferred by RNA-seq. (B) The nucleotide sequence alignment of the upstream region of the exon L. The start codon of the exon L is indicated. Lizard, *Anolis carolinensis*; Alligator, *Alligator mississippiensis*; Turtle, *Pelodiscus sinensis*.

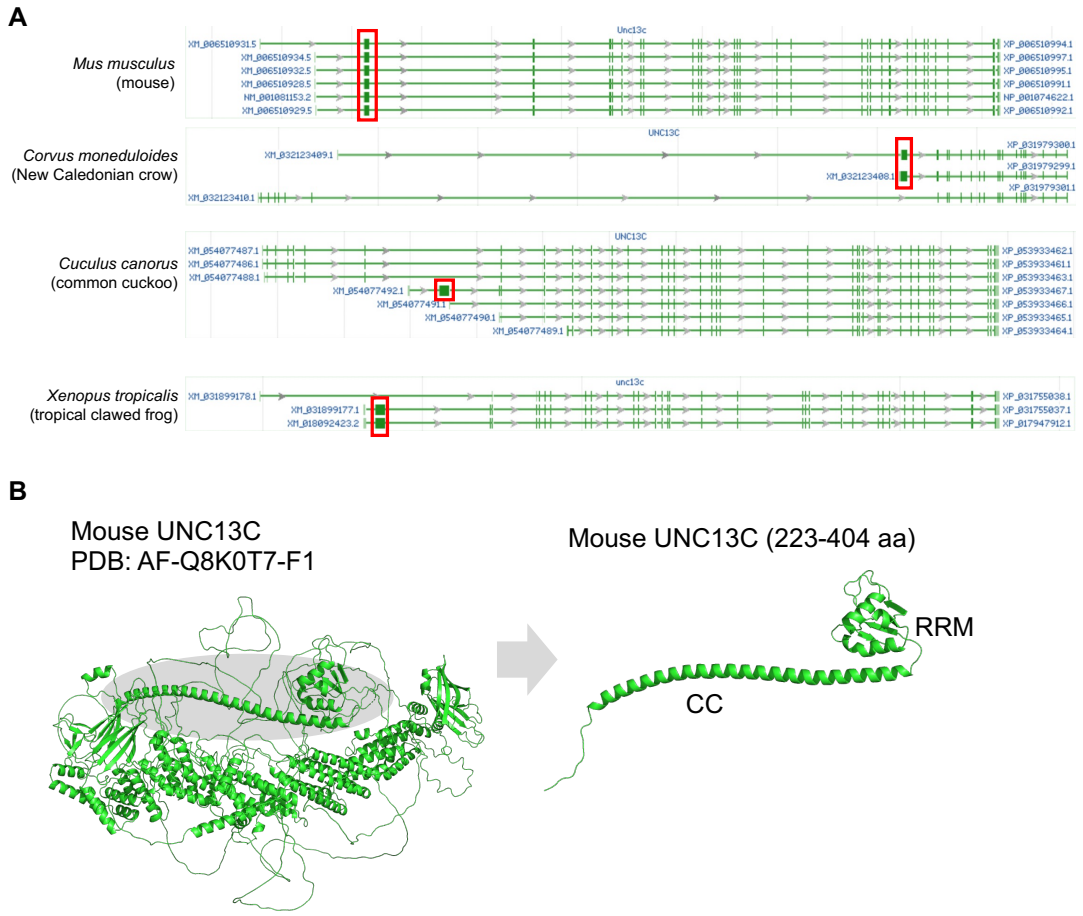


**Figure S8. A canonical exon of *UNC13C* encodes a protein similar to L1 ORF1p.** (A) Exons encoding ORF1p-like amino acids are enclosed in squares. In mouse, all splicing variants of *Unc13c* contain the exon encoding ORF1p-like amino acids. In the three species below, splicing variants without ORF1p-like exons are annotated. (B) The 3D structure of mouse UNC13C predicted by AlphaFold2 (PDB: AF-Q8K0T7-F1). On the left is the predicted structure of full-length UNC13C, while on the right is the partial structure corresponding to the L1 ORF1p-like region. CC, coiled-coil; RRM, RNA recognition motif.